UNITED NATIONS EDUCATIONAL, SCIENTIFIC AND CULTURAL ORGANIZATION
INTERNATIONAL ATOMIC ENERGY AGENCY
INTERNATIONAL CENTRE FOR THEORETICAL PHYSICS
I.C.T.P., P.O. BOX 586, 34100 TRIESTE, ITALY, CABLE: CENTRATOM TRIESTE

H4.SMR/1058-20

WINTER COLLEGE ON OPTICS

9 - 27 February 1998

The Characterization of Laser Beams

A. Sona

CISE, Milano, Italy

Winter College on Optics

Conference on Laser Beams Characterization

by Alberto Sona

Outline :

* Motivation and examples
* Beams focusability and spatial coherence
* The M^2 approach : a beam invariant
* The second order momentum of I(x,y)
* Alternative simpler approaches : slit, knife edge ,variable aperture
* Gaussian beams single and multimode.
* Instruments for measuring I(x,y) and M^2
* Results of a round robin test.
* The modal content and the inversion problem.
* Wavefront phase measurements.
* Other beam parameters considered by the Norms.

Trieste, February 1998

BEAM FOCUSING PARAMETERS

radius $S = K \lambda (f/D)$

$K = 1.22$ plane wave @ 1st Bessel zero

$K = 2/\pi$ gaussian beam @ $\frac{1}{e^2}$ Int

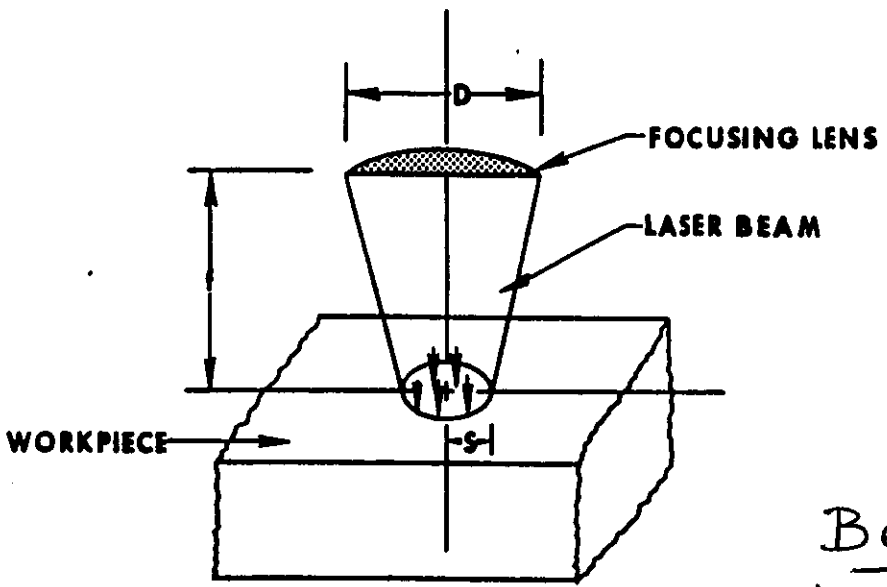

THEORETICAL MINIMUM SPOT RADIUS:

$$S = 1.22\,(\lambda)\left[\frac{f}{D}\right]$$

84% OF BEAM ENERGY WITHIN THIS RADIUS FOR UNIFORM PLANE WAVE IMPINGING ON FOCUSING LENS

Beam parameter

$$1/M^2 = K = B_p = \frac{\lambda}{\pi \cdot \theta w} = 1 \quad \text{for TEM}_{00} \quad (*)$$

Depth of focus (50% intensity) $Z_{0.5} = \pm \frac{4\lambda}{\pi}\left(\frac{f}{D}\right)^2$

gaussian beam diameter D at $1/e^2$ points

(*) $B_p = (2p + \ell + 1)^{-1}$ (Laguerre); $B_p = (2m+1)^{-1}$ (Hermite)

circular coordinates rectangular coordinates

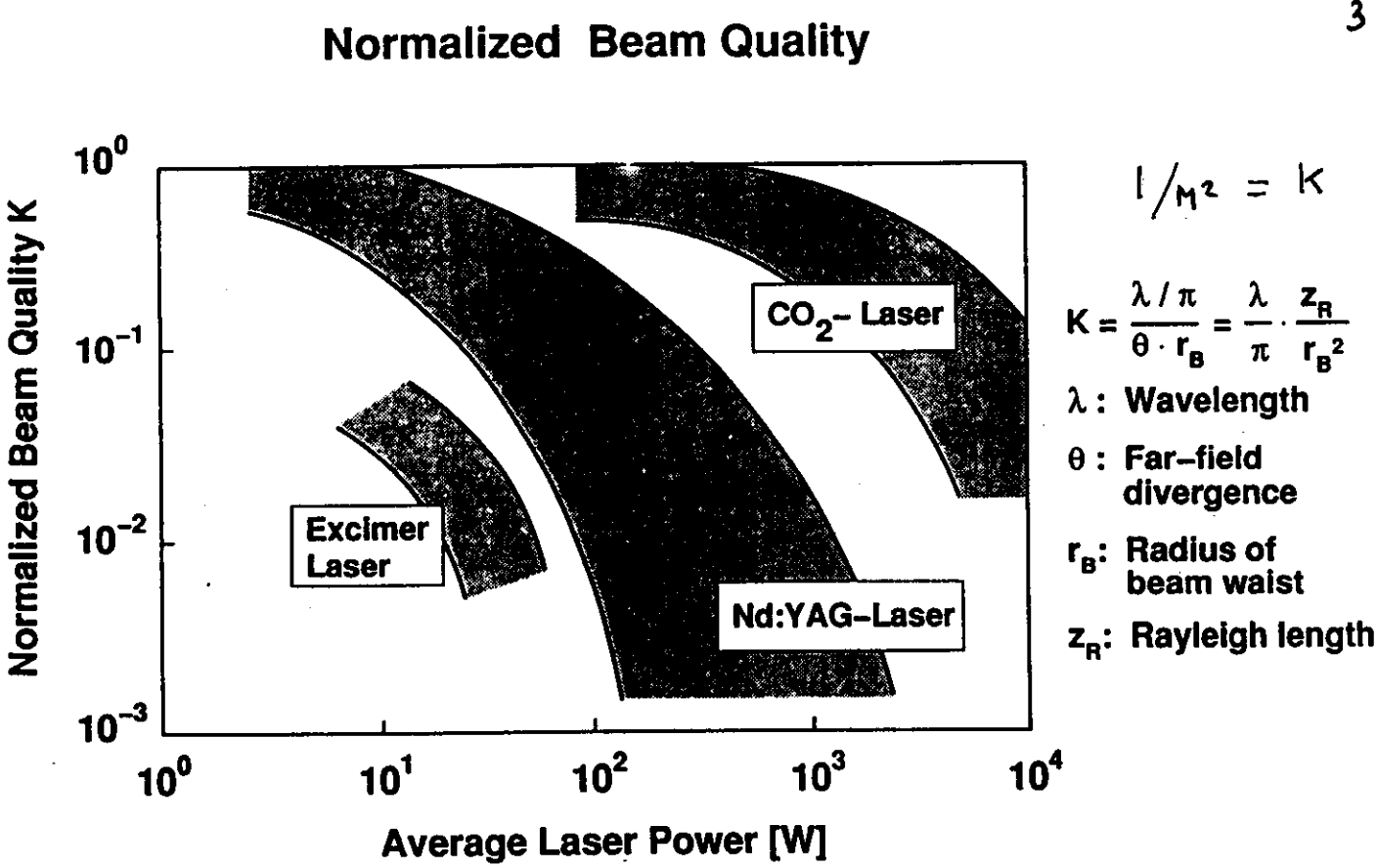

FIGURE 1

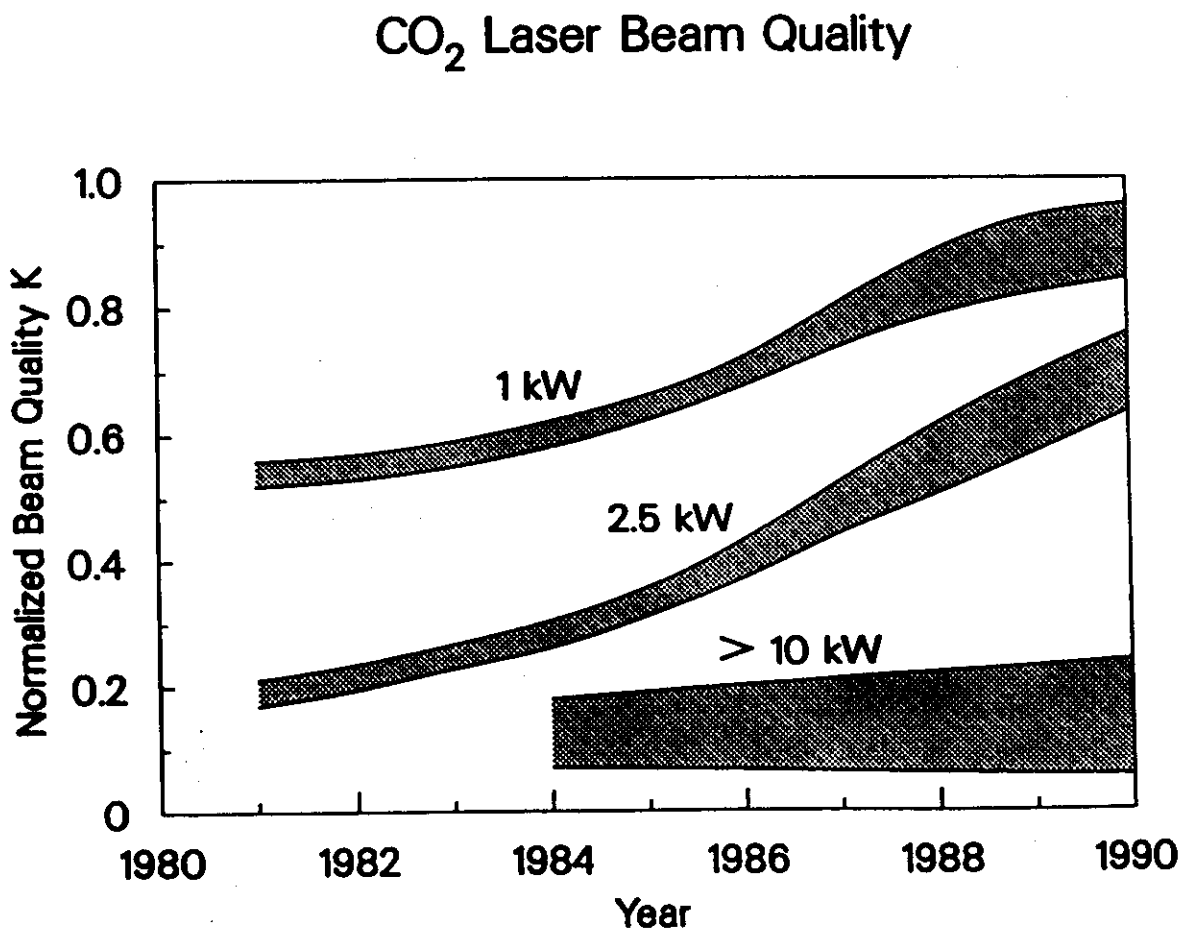

FIGURE 2

Spatial Coherence & Directionality

- First order correlation function between the field amplitudes at the same time in different points {ensemble (or time) ave.}

$$\Gamma_{12}^{(1)}(\bar{r}_1-\bar{r}_2,t) = \langle E_1(\bar{r}_1,t)\, E_2^*(\bar{r}_2,t)\rangle$$

- The normalized function is called the "degree of spatial coherence defined as:

$$\gamma_{12}^{(1)}(\bar{r}_1-\bar{r}_2,0) = \Gamma_{12}^{(1)}(\bar{r}_1-\bar{r}_2,0) \Big/ \left\{\Gamma_{11}^{(1)}(\bar{r}_1)\cdot\Gamma_{22}^{(1)}(\bar{r}_2)\right\}^{1/2} \leq 1$$

(in general is a complex quantity)

- The value $|\bar{r}_1-\bar{r}_2|$ for which $|\gamma_{12}^{(1)}(\bar{r}_1-\bar{r}_2,0)| = 1/2$ defines the "coherence radius and the related "coherence area".

- For an ideal unlimited wave (f.i. coming from a single spatial mode of a Laser) the coherence radius $\to \infty$.

NF Near Field
- For a wavefront limited by an aperture with a diameter D the propagation vector $\bar{K}$ is affected by a spread $\Delta K = K \cdot \Delta\theta$ where $\Delta K = 1.22 \cdot 2\pi/D$.

FF Far Field
- If the apertured beam is focused by a lens of focal length f the spot size is defined by $\Delta s = f\,\Delta\theta = f \cdot 1.22\,\lambda/D$ and again the limitation due to diffraction holds: $\frac{1}{\lambda}\cdot\frac{D}{f} = \frac{1}{\lambda}\frac{\Delta K}{K} = \frac{\Delta K}{2\pi} = 1.22/\Delta s$

$\left(\frac{D}{f} = \frac{\Delta K}{K} = \frac{K\,\Delta\varphi^{FF}}{K} = F\text{-number}\right)$

The space concentration limit is

$$\boxed{\Delta s \simeq 1.22\,\frac{f}{D}\,\lambda}$$ (a few λ's).

Spatial Coherence & Directionality

Young Interferometer:

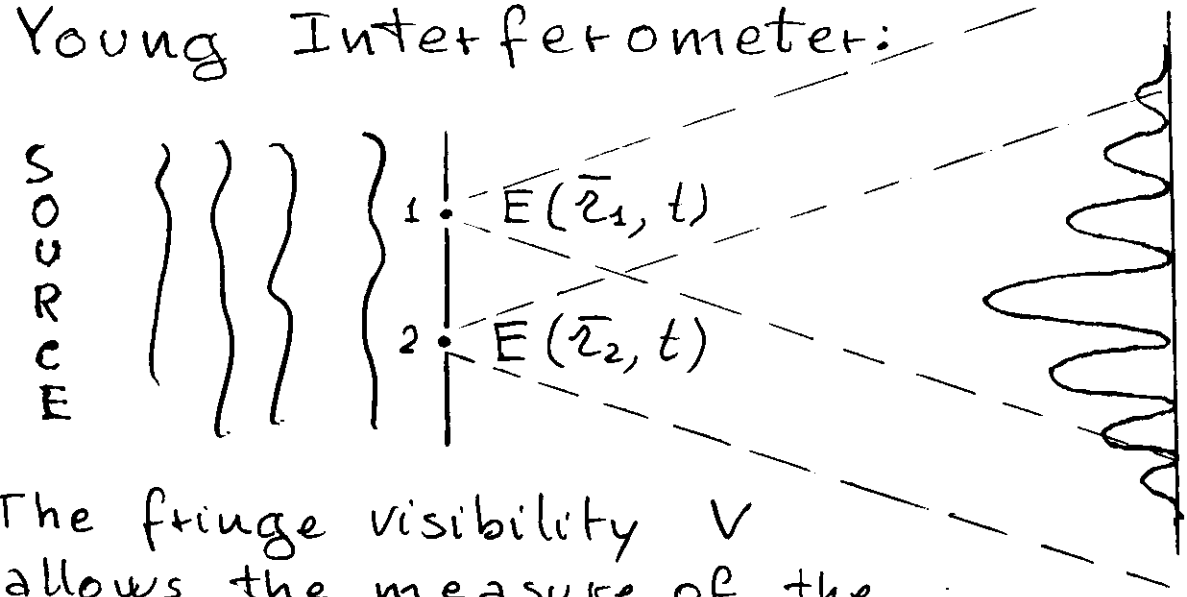

The fringe visibility V allows the measure of the "coherence radius" and "coherence area"

Beams with partial spatial coherence have a divergence greater than for a spatially coherent beam with the same intensity distribution.

Example: Semiconductor lasers or solid state lasers with "hot spots"

The divergence is $\theta'_d \simeq 1.22\ \lambda/d$ instead of $\theta_D \simeq 1.22\ \lambda/D$

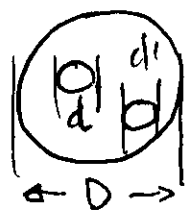

Multimode lasers have a divergence larger than the single mode case.

$$\theta_{e,m} = C_{e,m} \cdot \frac{\lambda}{\pi w_0}$$

$C_{em} > 1.16$

$C_{00} \simeq 1.16$

(if the spot size $\equiv$ 90% of beam power is considered)

The lack of spatial coherence reduces the fringe visibility and consequently the efficiency f.i. of an hologram

HIGHER-ORDER GAUSSIAN MODES

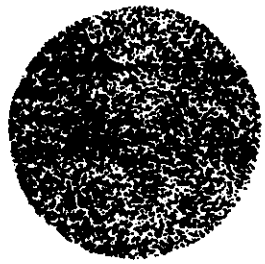

pl = 0, 0

0, 3

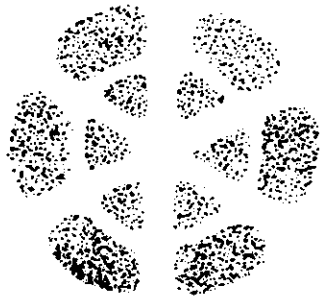

1, 3

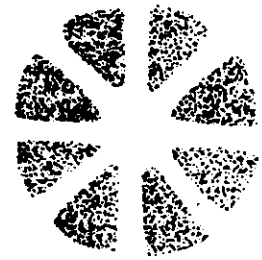

0, 4

Transverse mode patterns for Laguerre-gaussian modes of various orders.

$M^2 = (2p + l + 1)$

p radial

l tangential

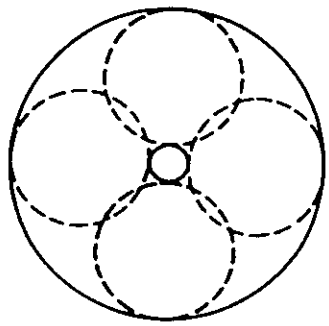

The "donut" mode is a linear superposition of 10 and 01 Hermite-gaussian modes.

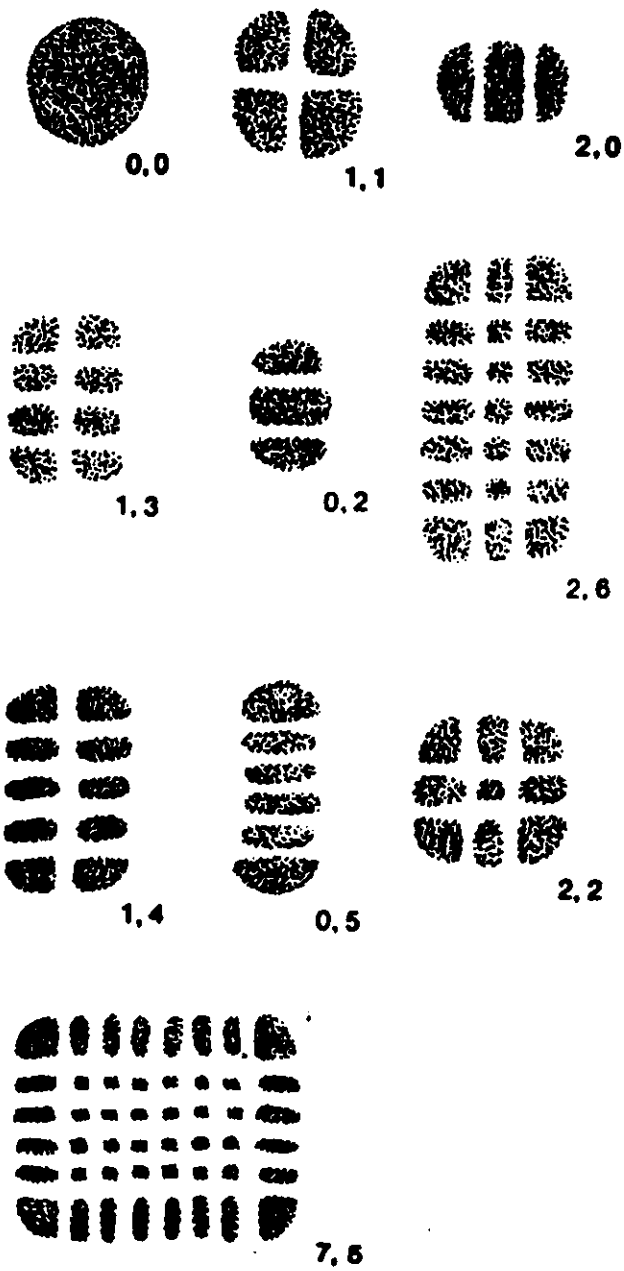

Transverse mode patterns for Hermite-gaussian modes of various orders.

$M_x = (2m+1)$; $M_y = (2n+1)$

First Moments (Centers of Gravity):

$$\iint_{-\infty}^{\infty} I(x,y)\,dx\,dy = \iint_{-\infty}^{\infty} \hat{I}(s_x, s_y)\,dx\,dy = 1$$

$$\bar{x}(z) \equiv \int\int x\, I(x,y,z)\,dx\,dy$$

$$\bar{y}(z) \equiv \int\int y\, I(x,y,z)\,dx\,dy$$

$$\begin{cases} \tilde{E}(x,y,z) = \mathcal{F}\left[\tilde{P}(s_x, s_y, z)\right] \;;\; I(x,y,z) = \left|\tilde{E}(x,y,z)\right|^2 \\ \tilde{P}(s_x, s_y, z) = \mathcal{F}^{-1}\left[\tilde{E}(x,y,z)\right] \;;\; \hat{I}(s_x, s_y, z) = \left|\tilde{P}(s_x, s_y, z)\right|^2 \end{cases}$$

$$\bar{s}_x \equiv \int\int s_x\, \hat{I}(s_x, s_y, z)\,ds_x\,ds_y$$

$$\bar{s}_y \equiv \int\int s_y\, \hat{I}(s_x, s_y, z)\,ds_x\,ds_y$$

$$2\pi s_x = K \sin\theta_x = \frac{2\pi \sin\theta_x}{\lambda} \;;\; s_x = \frac{\sin\theta_x}{\lambda} \approx \frac{\theta_x}{\lambda}$$

s_x, s_y Spatial Frequencies

$$s_y = \frac{\sin\theta_y}{\lambda} \approx \frac{\theta_y}{\lambda}$$

Second Moments (Variances):

$$\sigma_x^2(z) \equiv \int\int (x - \bar{x})^2 \; I(x, y, z) \; dx \, dy$$

$$\sigma_y^2(z) \equiv \int\int (y - \bar{y})^2 \; I(x, y, z) \; dx \, dy$$

$$\sigma^2(z) = \sigma_x^2(z) + \sigma_y^2(z)$$

$$\sigma_{s_x}^2 \equiv \int\int (s_x - \bar{s}_x)^2 \; \hat{I}(s_x, s_y, z) \; ds_x \, ds_y$$

$$\sigma_{s_y}^2 \equiv \int\int (s_y - \bar{s}_y)^2 \; \hat{I}(s_x, s_y, z) \; ds_x \, ds_y$$

$$\sigma_s^2 = \sigma_{sx}^2 + \sigma_{sy}^2$$

Definition of M^2 (Beam quality):

$$\sigma_{0x}\sigma_{s_x} \equiv \frac{M_x^2}{4\pi} \qquad \text{and} \qquad \sigma_{0y}\sigma_{s_y} \equiv \frac{M_y^2}{4\pi}$$

$1/K_x = M_x^2 \equiv 4\pi\,\sigma_{0x}\sigma_{sx}$; $1/K_y = M_y^2 = 4\pi\,\sigma_{0y}\sigma_{sy}$

$$M_x^2 \equiv \frac{(\text{Beamwidth-beamspread product})_{Real\,beam}}{(\text{Beamwidth-beamspread product})_{TEM_{\infty}}}$$

$$M_y^2 \equiv \frac{(\text{Beamwidth-beamspread product})_{Real\,beam}}{(\text{Beamwidth-beamspread product})_{TEM_{\infty}}}$$

$$M_x^2 \geq 1 \qquad \text{and} \qquad M_y^2 \geq 1$$

- $M_r^2 = 2\pi\,\sigma\,\sigma_\theta$

For a TEM_{00} Gaussian Beam:

$$\sigma_{0x} = \sigma_{0y} = \frac{w_0}{2} \qquad \text{and} \qquad \sigma_{s_x} = \sigma_{s_y} = \frac{1}{2\pi w_0}$$

$$M_x^2 = M_y^2 = 1 = 4\pi\,\frac{w_0}{2}\cdot\frac{1}{2\pi w_0}$$

$K_x = \frac{1}{M^2_x}$; $K_y = \frac{1}{M^2_y}$;

M^2 Properties:

- M^2 is a characteristic of the beam and remains constant after propagation through any non aberrated optical system

- This theory is rigorously valid for any beam

- These Propagation formulas reduce to the ordinary ones if the beam is gaussian

- Analogous formulas are in cylindrical coordinates for circular symmetric beams

Definitions: (according to the Norms)

σ - from the second polar moment $M^2 = M_x^2 + M_y^2$

σ_x, σ_y - from the second moments with respect to axis x and y (M_x^2 ; M_y^2)

$$\begin{cases} d_\sigma = 2\sqrt{2}\,\sigma = 2\sqrt{2}\,\dfrac{w}{\sqrt{2}} = 2w \;;\; \sigma = \dfrac{w}{\sqrt{2}} \\ d\sigma_x = 4\,\sigma_x = 4\,\dfrac{w_x}{2} = 2w_x \;;\; \sigma_x = \dfrac{w_x}{2} \\ d\sigma_y = 4\,\sigma_y = 4\,\dfrac{w_y}{2} = 2w_y \;;\; \sigma_y = \dfrac{w_y}{2} \end{cases}$$

$\boxed{\sigma^2 = \sigma_x^2 + \sigma_y^2}$; **In the case of a beam with circular symmetry** $\begin{cases} w_x = w_y = w \\ d\sigma_x = d\sigma_y = d\sigma \end{cases}$

In a similar way :

$$\begin{cases} \theta_\sigma = 2\sqrt{2}\,\sigma_\theta = 2\sqrt{2}\,\dfrac{\sqrt{2}\,\lambda}{2\pi w_0} = \dfrac{2\lambda}{\pi w_0} \;;\; \sigma_\theta = \dfrac{\lambda}{\sqrt{2}\pi w_0} \\ \theta_{\sigma x} = 4\,\sigma_{\theta x} = 4\,\dfrac{\lambda}{2\pi w_0} = \dfrac{2\lambda}{\pi w_0} \;;\; \sigma_{\theta x} = \dfrac{1}{2\pi}\dfrac{\lambda}{w_0} \\ \theta_{\sigma y} = 4\,\sigma_{\theta y} = 4\,\dfrac{\lambda}{2\pi w_0} = \dfrac{2\lambda}{\pi w_0} \;;\; \sigma_{\theta y} = \dfrac{\lambda}{2\pi w_0} \end{cases}$$

$\boxed{\sigma_\theta^2 = \sigma_{\theta x}^2 + \sigma_{\theta y}^2}$

$\dfrac{2\pi}{\lambda}\sigma\theta_\sigma = \dfrac{1}{k} = \boxed{M_r^2 = \dfrac{\pi}{4\lambda}\, d_\sigma\, \theta_\sigma} = \dfrac{\pi}{4\lambda}\, 2w_0 \cdot \dfrac{2\lambda}{\pi w_0} = 1$ (Per il TEM$_{00}$)

$\dfrac{1}{k_x} = M_x^2 = \dfrac{\pi}{4\lambda}\, d_{\sigma x}\, \theta_{\sigma x} = 1$;

The relationship between M_r , M_x , and M_y is given by :

$$\boxed{M_r^4 = \left(\frac{\sigma_{\theta x}^2 + \sigma_{\theta y}^2}{4\,\sigma_{\theta x}^2}\right) M_x^4 + \left(\frac{\sigma_{\theta x}^2 + \sigma_{\theta y}^2}{4\,\sigma_{\theta y}^2}\right) M_y^4}$$

in the absence of astigmatism.

$\frac{1}{e^2}$

$x_1 \Rightarrow$ 13.5 % ; $x_2 =$ 13.5 % $\quad d_s = x_2 - x_1$

$$d_\sigma = d_s \frac{1}{M_s^2} \left(0,95 (M_s^2 - 1) + 1\right)$$

for $M_s^2 = 1 \quad d_\sigma = d_s$

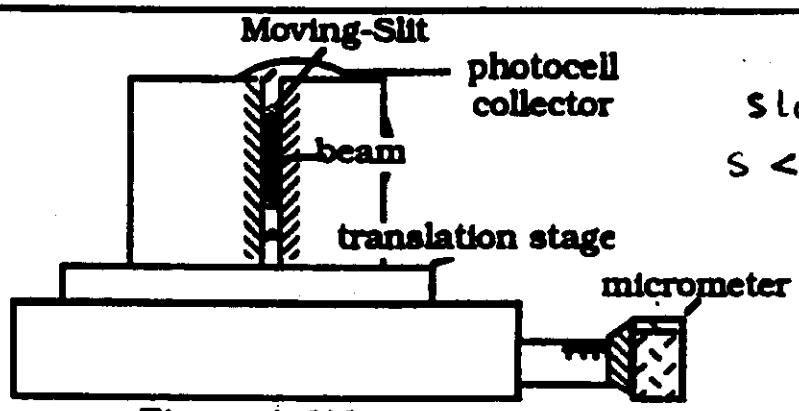

Slit width $s < \frac{1}{20} d_s$

Figure A.1.1.a
Moving Slit Beam Width Measuring Device

$1 - e^{-2} =$ 86.5 % of the total power

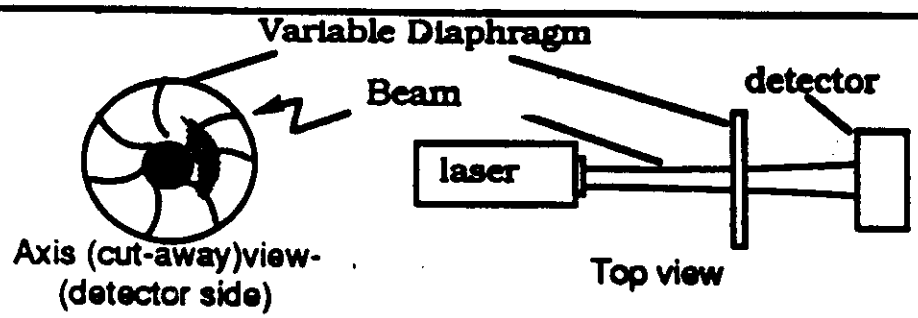

Figure A.3.1.a.

$$d_\sigma = d_{86.5} \frac{1}{M_{86.5}^2} \left(1.14 (M_{86.5}^2 - 1) + 1\right)$$

for $M_{86.5}^2 = 1 \quad d_\sigma = d_{86.5}$

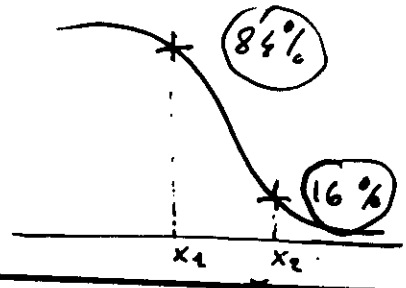

$$d_K = 2(x_2 - x_1)$$

$$d\sigma = d_K \frac{1}{M_K^2}\left(0{,}81(M_K^2 - 1) + 1\right)$$

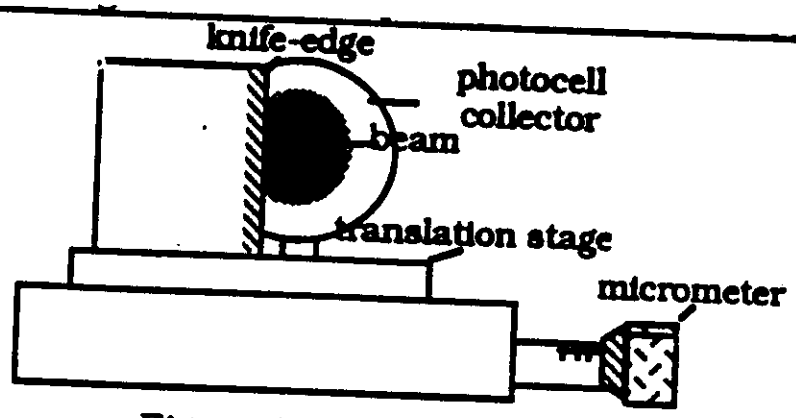

Figure A.2.1.a
Moving Knife Edge
Beam Width Measuring Device

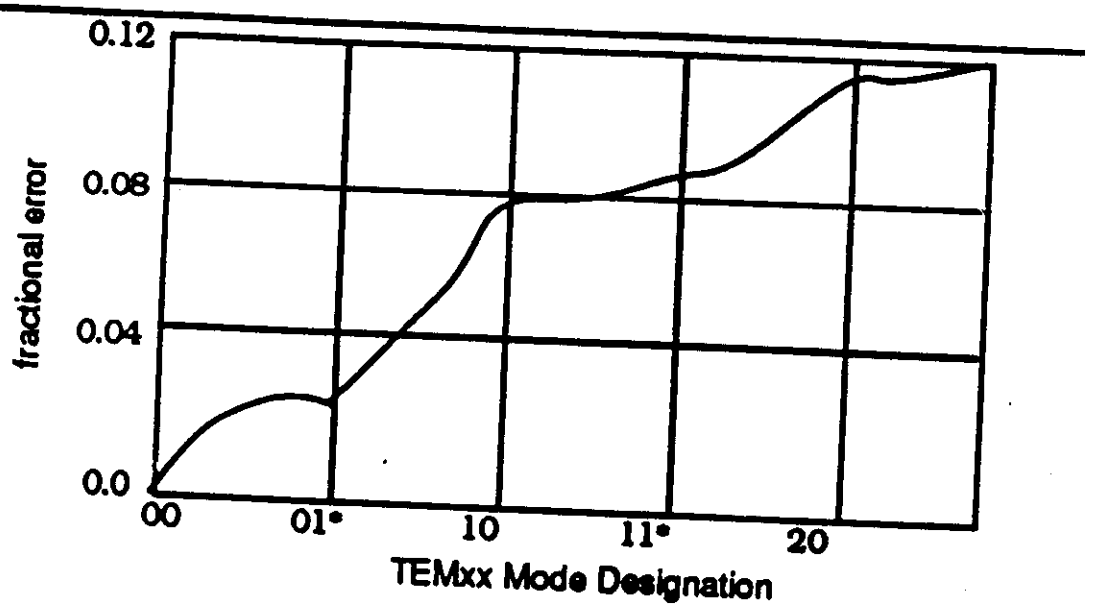

Figure A.2.1.b
Moving Knife-Edge: Fractional Error in
Diameter Measurement Of
Laguerre-gaussian Modes

Comments on the M^2 approach

* Problems for the measurements are present in the following cases :

  * In pulsed lasers M2 is in general time dependent ; only averages value can be derived in a simple way.
  * Annular beams generated by unstable resonators have always $M^2 > 1$.(i.e the meaning of "times diffraction limited" is no more valid)
  * Non Gaussian beams or non paraxial beams can give rise to large errors.
  * Asymmetric or two lobes beams (f. i. from semiconductor lasers) also need special data processing.
  * The measurement of I(x,y) exploits the w (z) expression to derive the beam waist size and location and the beam divergence .
  * Additional information could be achieved by using the expression of R(z) in connection with wavefront phase measurements.

To derive a better information on the modal content joint I(x,y) and phase measurements could be of use.

New instruments would be welcome providing information on the spatial coherence of the beam cross section by phase measurements.

Extract of the ISO/TC 172/SC 9 work programme, listing items dealing with test methods for laser beam parameters

ISO Work Item	Title
11146	Test methods for laser beam parameters: Beam widths, divergence angle and beam propagation factor
11554	Test methods for laser beam parameters: Power, energy and temporal characteristics
11670	Test methods for laser beam parameters: Beam positional stability
12005	Test methods for laser beam parameters: Polarization
13694	Test methods for laser beam parameters: Power (energy) density distribution
13695	Test methods for laser beam parameters: Spectral characteristics
15367	Test methods for laser beam parameters: Phase distribution

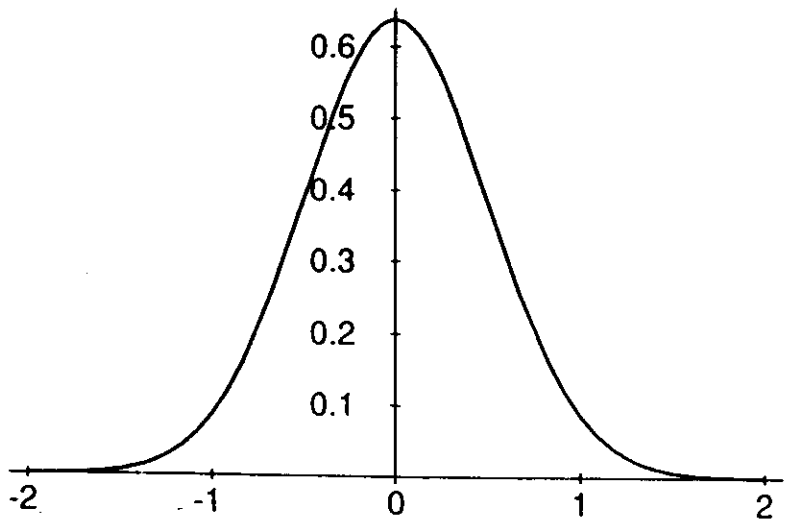

Intensity profile for a pure gaussian TEM_{00} beam.

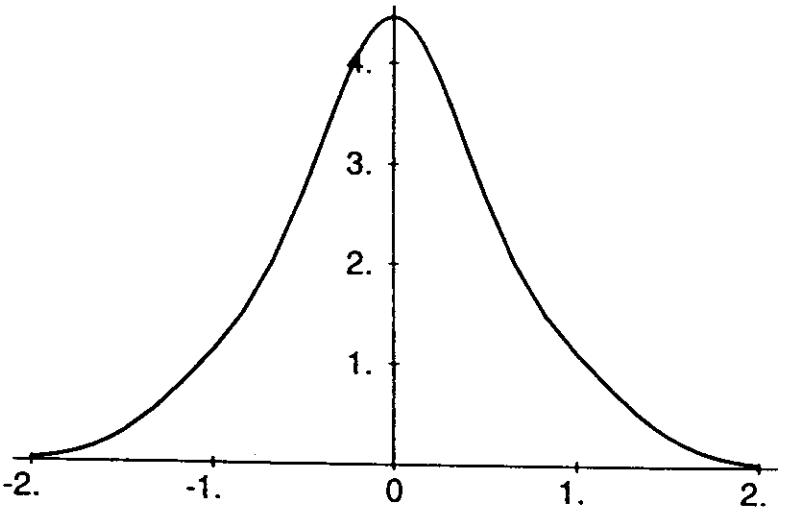

Intensity profile for a beam made up of 50% TEM_{00}, 30% TEM_{01}, and 20% TEM_{10} Laguerre-gaussian modes.

Beam profile comparisons

Laguerre-Gauss Modes

$$M_{\cdot}^2 = (2p + l + 1)$$

p radial
l tangential

Laser Mode p l	M2
TEM 00	1
TEM 01*	2
TEM 10	3
TEM 11*	4
TEM 20	5
TEM 21*	6

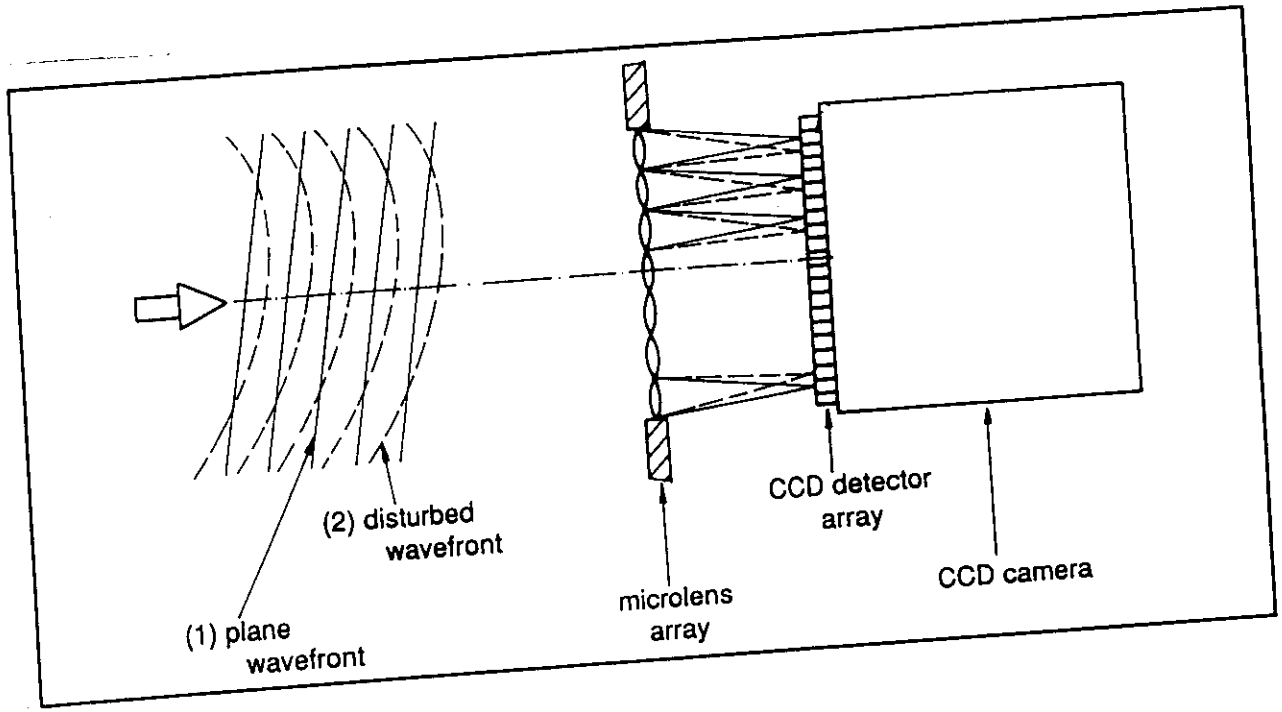

Fig. 1: Operating principle of the Shack-Hartmann wavefront sensor

- high sensitivity of gradient measurement (> λ/250 across each subaperture at λ = 633 nm)
- wide dynamic range (14 λ per subaperture at λ = 633 nm)
- no scanning procedure required
- simultaneous recording of the wavefront
- both continuous and pulsed exposure
- extremely high-speed exposure
- no movable mechanical parts
- sturdiness and vibration resistance
- straightforward optical adaptation
- no special demands on
  - the light source and its spectral properties (both incoherent and coherent light can be used)
  - the spectral bandwidth (freely selectable)
- easy integration
- easy alignment and calibration
- alignment stability
- high thermal stability
- immediate readiness for use

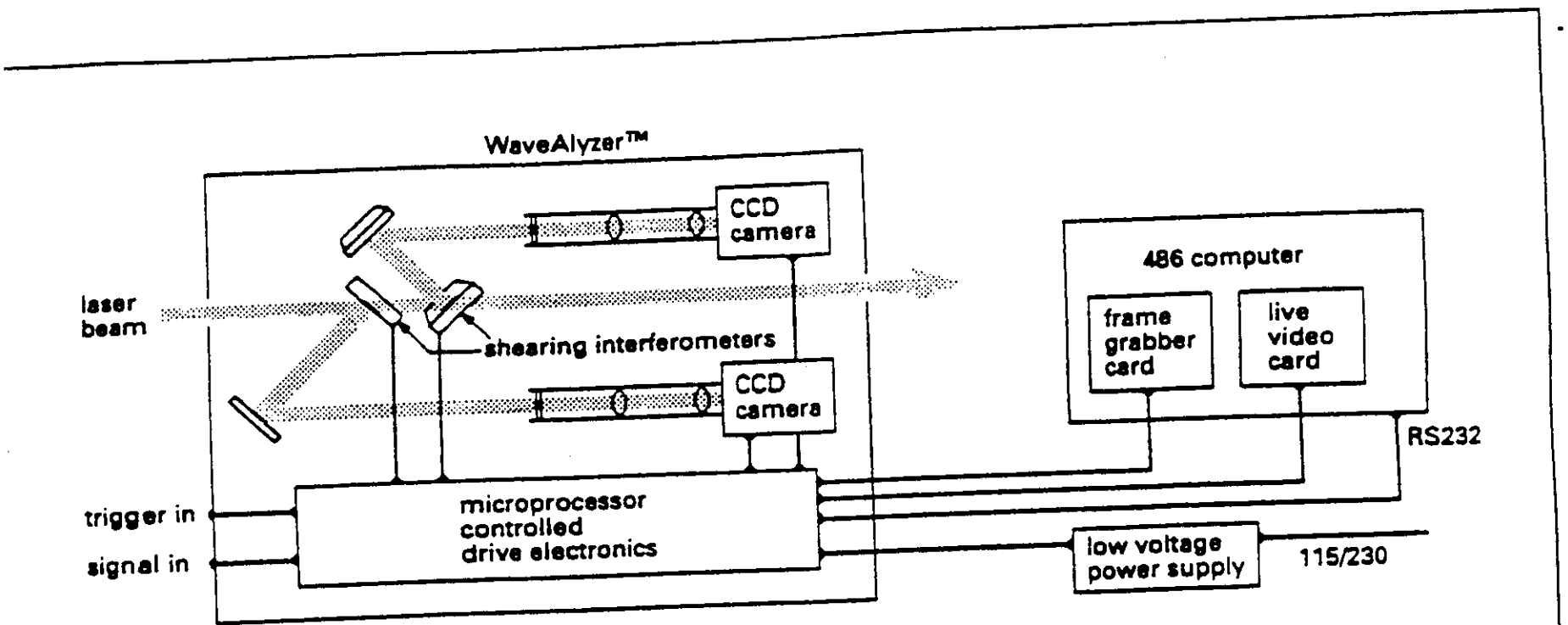

Figure 4. Layout of the wavefront analyzer system. The optical paths for the two interferometers are shown in the same plane for clarity, but are actually in orthogonal planes.

Zernike or (better) Kingslake

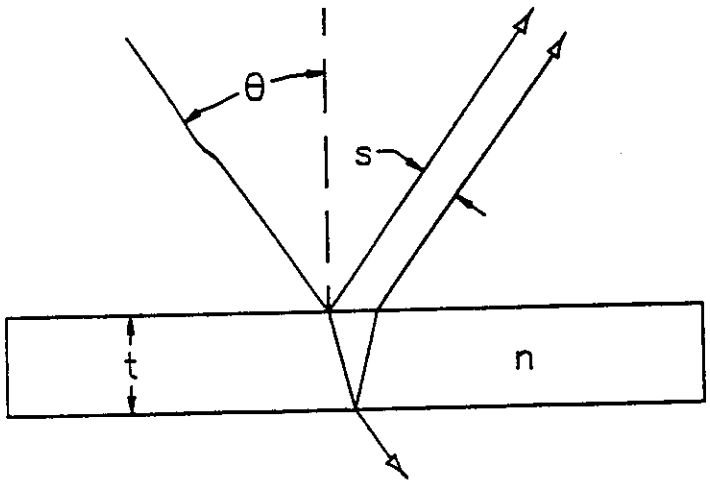

Figure 1. Geometry of a shearing interferometer. An incident ray at angle θ is reflected by the plane, parallel front and back surfaces of the etalon. The two reflected rays are sheared an amount s.

Dynamic Shearing:

$$s = \frac{t \sin\theta}{\sqrt{n^2 - \sin^2\theta}}$$

$$d = 2t\sqrt{n^2 - \sin^2\theta}$$

$$\frac{\partial d}{\partial \theta} = \frac{-t \sin\theta \cdot 2}{\sqrt{n^2 - \sin^2\theta}} = -s$$

Ex $\Delta\theta = \frac{\Delta d}{s} = \frac{0.633}{750} = 8.44$ mr

@ θ = 50°

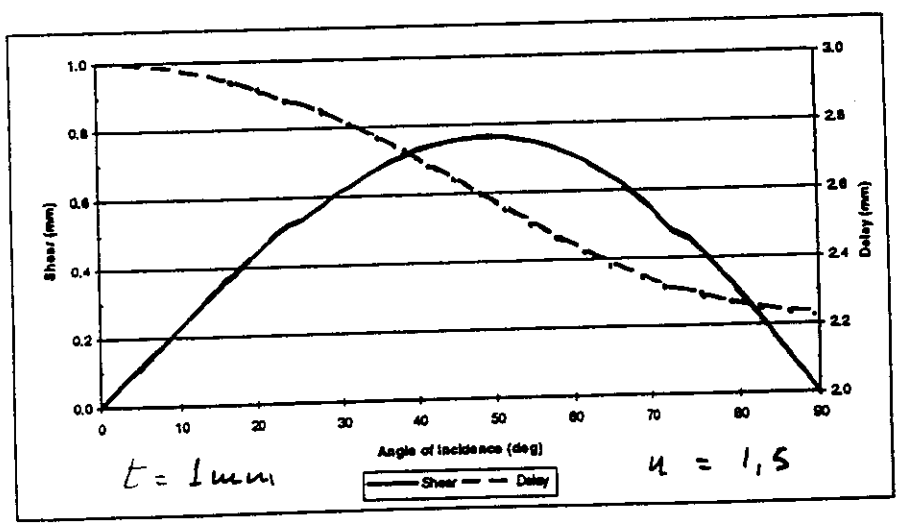

Figure 2. Shear and delay of a 1 mm thick etalon with index of refraction of 1.5 as a function of incidence angle. Note that the maximum shear is at an incidence angle of about 50°.

R radius of curvature

Pitch of fringe $\Lambda = R\frac{\lambda}{s}$

spherical